Interspecies interactions in bacterial colonies are determined by physiological traits and the environment

Running Title

Interspecies interactions in bacterial colonies

Authors

Sean C. Booth[1†] and Scott A. Rice[1,2,3]

[1]The Singapore Centre for Environmental Life Sciences Engineering and [2]The School of Biological Sciences, Nanyang Technological University, Singapore

[3]The ithree Institute, The University of Technology Sydney, Australia

[†]Current address: Department of Zoology, University of Oxford, UK

Corresponding author: RSCOTT@NTU.EDU.SG, +65 65927944

Abstract

Interspecies interactions in bacterial biofilms have important impacts on the composition and function of communities in natural and engineered systems. To investigate these interactions, synthetic communities provide experimentally tractable systems. Agar-surface colonies are similar to biofilms and have been used for investigating the eco-evolutionary and biophysical forces that determine community composition and spatial distribution of bacteria. Prior work has focused on intraspecies interactions, using differently fluorescent tagged but identical or genetically modified strains of the same species. Here, we investigated how physiological differences determine the community composition and spatial distribution in synthetic communities of *Pseudomonas aeruginosa*, *Pseudomonas protegens* and *Klebsiella pneumoniae*. Using quantitative microscopic imaging, we found that

interspecies interactions in multispecies colonies are influenced by type IV pilus mediated motility, extracellular matrix secretion, environmental parameters and the specific species involved. These results indicate that the patterns observable in mixed species colonies can be used to understand the mechanisms that drive interspecies interactions, which are dependent on the interplay between specific species' physiology and environmental conditions.

Keywords: Pseudomonas, Klebsiella, biofilm, colony, interspecies interactions, model community

Introduction

The growth and survival of bacteria in natural and engineered systems is strongly influenced by how they interact with one another [1, 2]. Interactions between community members vary considerably; some interactions facilitate growth and survival, while others inhibit growth or even result in the death of one species [3]. Both faciliatory and inhibitory interactions can be mediated by secreted products, e.g. metabolite exchange [4] and antibiotic production [5] or by contact-dependent mechanisms, e.g. adhesion [6, 7] and Type VI secretion mediated killing [8]. Regardless of the specific mechanism of interaction, the composition and function of a community is influenced by the combination and sum of the various interactions between its constitutive members [9, 10].

Studies of the interactions between community members have shown how interspecies interactions influence community-intrinsic properties [11]. While competitive interactions between individual species are expected and common [12], often due to overlap of metabolic preferences [13], cooperative interactions can also be found in larger communities which enable increased biomass production [14] or resistance to antimicrobial agents [15]. Biofilms are ideal for examining the effect of interactions on a community, as cells are in close proximity to each other and are embedded within self-secreted biofilm matrix [16, 17]. For example, biofilms have been used to show how the genetic division of labor improves pellicle formation [18] and that spatial structure influences the evolution [19], formation [20] and outcome [21] of interspecies interactions. Using a synthetic, three-species community, we have shown that co-culture biofilms exhibit increased growth by particular members and enhanced stress tolerance for the entire community [22]. This occurred despite the community members competing for the same resources and was not observed for planktonic mixed cultures, suggesting that spatial organization within biofilms is important for species interactions.

51 Colonies grown on a nutrient surface are an efficient system for manipulating and
52 visualizing the spatial distribution of different microorganisms, but have mostly been used for
53 studying eco-evolutionary dynamics [23]. They have been used to characterize various
54 spatiotemporal aspects of microbial interactions including the co-localization of mutually
55 auxotrophic strains of *Saccharomyces cerevisiae* [24, 25], the vertical separation of differently
56 sized cells of *Escherichia coli* [26], the sequential range expansion of nitrate reducing
57 *Pseudomonas stutzeri* [27], the spatial separation patterns of strains of *Vibrio cholerae* [28] or
58 *Bacillus subtilis* [29] that differ in the quantity of extracellular matrix produced, and the
59 proportion of different antibiotic resistant/sensitive strains of *P. aeruginosa* [30]. All of these
60 studies have focused on different strains or mutants of a single species (intraspecies
61 interactions), differing only in the fluorescent marker they express and targeted deletion of
62 specific genes. However, it is also clear that this approach has considerable potential for
63 investigating interactions between different species.

64 In this study, we investigated the interactions between members of a model community
65 consisting of *P. aeruginosa* PAO1, *P. protegens* Pf-5 (formerly *P. fluorescens* [31, 32]) and *K.*
66 *pneumoniae* KP-1. These species can be commonly found in soils and habitats as varied as
67 metalworking fluid or the gut of silk moths [33, 34]. When co-cultured in flow-cell biofilms,
68 this community exhibits properties not observed in biofilms of the individual species or liquid
69 cultures including a relative increase in *K. pneumoniae*, sharing of resistance to sodium dodecyl
70 sulfate allowing the sensitive species, *P. protegens*, to survive, [22] and reduced production of
71 morphotypic variants for all species [35]. As colonies offer some advantages compared to flow-
72 cell biofilms, including higher throughput and the ability to image the entire colony, here we
73 assessed interactions between each possible pair of these species by co-culturing them in a
74 colony biofilm model. We determined whether these interactions were beneficial or detrimental
75 by quantifying the area colonized by each species and qualifying where each species was found.

76 By manipulating the community through using mutant strains and/or altered environmental
77 conditions, we also show how organism-specific physiology determines interaction outcomes.
78 This approach thus has the potential to identify gene systems and environmental conditions
79 that underlie the interactions between bacteria. This work demonstrates that co-culturing in
80 colony biofilms is a useful tool for determining the outcome of interactions between bacteria
81 and visualizing the emergent properties of multi-species biofilms.
82

83 **Materials and Methods**

84 **Strains, media and growth conditions:** Colonies were grown on minimal medium (48 mM
85 Na_2HPO_4; 22 mM KH_2PO_4; 9 mM NaCl; 19 mM NH_4Cl; 2 mM $MgSO_4$; 0.1 mM $CaCl_2$; 0.04
86 mM $FeSO_4$; 2 mM glucose and 0.4% casamino acids) with either 1.5% or 0.6% agar in 24 well
87 plates or 8 well Ibidi™ slides. Previously described strains (Table 1) [22] of *P. aeruginosa*
88 PAO1, *P. protegens* Pf-5 and *K. pneumoniae* KP-1 constitutively expressing fluorescent
89 protein genes inserted into the chromosome using a Tn7 transposon were recovered from
90 freezer stocks directly onto LB agar plates and grown for 24-48 h at room temperature. Bacteria
91 were inoculated into liquid medium from agar plates (because they are highly mucoid, wild-
92 type *K. pneumoniae* strains were homogenized by passing repeatedly through a 30 G needle),
93 the OD_{600} was standardized to 0.1 and 1/100 dilutions were used directly or mixed 1:1 and 0.5
94 µL was spotted at the center of each well. Spots were dried for 30 min in a laminar flow cabinet,
95 plates were sealed with parafilm and incubated at room temperature. To confirm that mixtures
96 were equal, colony forming units (CFUs) were determined for the inoculum for each
97 species/strain. If CFU counts indicated that the ratio of two mixed species/strains was more
98 than 10 to 1 the sample was not used. For co-culture colonies, only combinations of CFP or
99 YFP labelled strains with dsRed or mCherry were used, with the exception of KP-1-YFP and
100 Pf-5-CFP, due to issues of overlapping excitation and emission spectra. When multiple

101 combinations were possible (e.g. KP-1-dsRed with KP-1-CFP or KP-1-YFP) both
102 combinations were treated as equivalent i.e. the combination of dsRed with CFP was
103 considered a replicate of combinations of dsRed with YFP.

104 Table 1: Species and strains used in this study.

Species and strain	Genotypic and phenotypic characteristics	Tn7 chromosomal fluorescent protein	Source or reference
P. aeruginosa PAO1	Wild-type	YFP, mCherry	ATCC BAA-47 [19], this study
P. aeruginosa PAO1 Small colony variant (SCV)	*pilT* Thr210 frameshift, twitching defect	YFP	[32]
P. protegens Pf-5	Wild-type	CFP, mCherry	ATCC BAA-477 [19], this study
K. pneumoniae KP-1	Wild-type	dsRed, CFP, YFP	[19]
K. pneumoniae KP-1 Non-mucoid variant (NMV)	UDP-glucose lipid carrier transferase Phe123Ile, matrix secretion defect	dsRed	[32]

105

106 **Image acquisition:** Colonies were imaged on a Zeiss Axio Observer.Z1 inverted (24 well
107 plates) or Imager.M2 upright (8 well slides) microscope using an HXP 120 C halogen light
108 source. On the Z1 a 5X/0.16 objective was used and a 10X/0.3 objective on the M2. The filter
109 sets (excitation/emission) used were: Zeiss Set 10 for CFP (450-490/515-565), Set 46 for YFP
110 (490-510/520-550) and Set 31 (550-580/590-660) for dsRed and mCherry on the Z1. Set 43

111 (520-570/565-630) was used for dsRed and mCherry on the M1. Exposure times and focus
112 were manually optimized for each sample then colonies were imaged using 'Tilescan' mode in
113 Zeiss Zen (Blue edition) with 10% overlap. Twelve-bit images were captured using an
114 AxioCamMRm3. Shading correction was applied using precaptured profiles of fluorescent
115 slides. Images from both microscopes were treated equivalently in downstream processing.
116 **Image Presentation:** Representative images from each experimental combination were
117 selected for presentation. Images were processed for viewing to improve contrast and remove
118 artefacts, but only raw images were used for quantitative analysis. Images were corrected for
119 flat-field illumination using BaSiC [36], stitched together in ImageJ [37, 38] and then the
120 brightness was scaled manually for each channel in each image. In cases when there was high
121 background signal, the background was either subtracted manually by segmenting the colony
122 area or by using the background subtraction tool.
123 **Image Analysis**: For full details, see the supplementary material. Briefly, tilescan images
124 stitched together using Zeiss Zen were imported into R and processed using the package
125 'imager' [39]. Each channel was normalized to a range of 0 to 1 and any background signal
126 was subtracted. To segment the colony from the background, a mask of the colony was
127 generated by taking the sum of all channels (including the inverted brightfield) then
128 thresholding this image using either "IJDefault" or "triangle" in the R package
129 'auto_thresholdr' [40]. To determine the amount of overlap between the two strains within a
130 colony, the ratio between channels was calculated at every pixel by subtracting one channel
131 from the other and dividing them by the sum of both ((c1-c2)/(c1+c2)). Thus, values can range
132 from 1/-1 indicating only the presence of one strain, to 0, indicating an exactly equal mix of
133 the two strains. The proportion of mixed pixels was then calculated by dividing the number of
134 bins in the range -0.25:0.25 by the total number of pixels within the colony as defined by the
135 segmentation. We then attempted to determine the area occupied by each strain within the

136 colony by thresholding each fluorescent channel with several different methods (including Li,
137 Huang and triangle), then manually selecting the most accurate method. Due to the manual
138 intervention required to pick an appropriate threshold, which varied substantially between
139 images, the area of each strain was instead manually determined in ImageJ. For all conditions
140 a minimum of 6 biological replicates were analyzed.

141 **Statistics:** Analysis of variance, Tukey's honest significant difference post-hoc test and
142 multiple-testing p-value adjustment were used to determine if there were significant differences
143 in colony area between single and dual species colonies.

144

145 **Results**

146 **Monospecies Colonies**

147 To compare patterns of interactions with previously published studies, we first
148 examined intraspecies interactions by growing colonies consisting of two strains of the same
149 species (Figure 1). Qualitative inspection of the colonies after 24 and 48 h of growth indicated
150 that each species differed in how they separate into sectors. *P. protegens* (Figure 1B,E) and *K.*
151 *pneumoniae* (Figure 1C,F) showed clear segregation between strains, although the shape of the
152 borders differed. For *P. aeruginosa* (Figure 1A,D), separation into sectors was only apparent
153 at 48 h and the borders between strains were less distinct than for the other species.

154 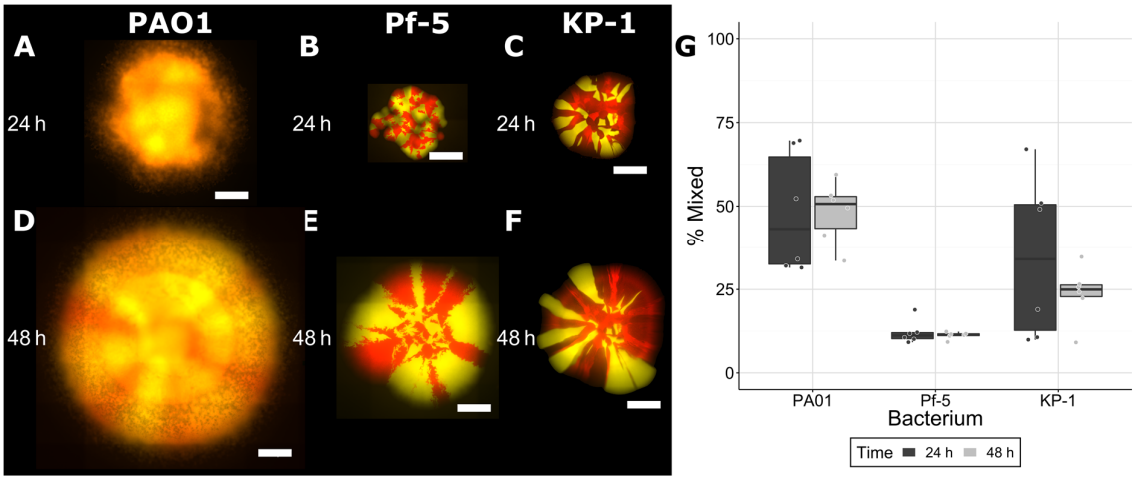

155 Figure 1: Colonies consisting of *P. aeruginosa* PAO1 (A, D), *P. protegens* Pf-5 (B, E) or *K.*
156 *pneumoniae* KP-1 (C, F). Each species was labeled separately with two different fluorescent
157 protein genes and are presented here as red or yellow (false colouring). Strains were mixed 1:1
158 (OD_{600}) at the time of inoculation and colonies were imaged after 24 and 48 h of growth. Scale
159 bars indicate 1000 µm. Overlap between strains was calculated from raw images as the
160 percentage of mixed pixels (G). Boxplots are presented in Tukey style.
161
162 To better characterize the differences in colony growth, quantitative analyses were
163 performed by determining the percentage of pixels with similar relative signal within each
164 colony (Figure 1, G). Around 50% of pixels were mixed in the *P. aeruginosa* colonies
165 compared to 25% or less in the other two species after 48 h of growth. Even at the leading edge
166 of *P. aeruginosa* regions that appeared to consist of a single strain, cells of both colours were
167 present and were well mixed (Supplementary Video 1). Movement and mixing of the two
168 strains was visible 500 µm inward from the colony edge (Supplementary Video 2). For all three
169 species, there was no change in mixing between 24 and 48 h.

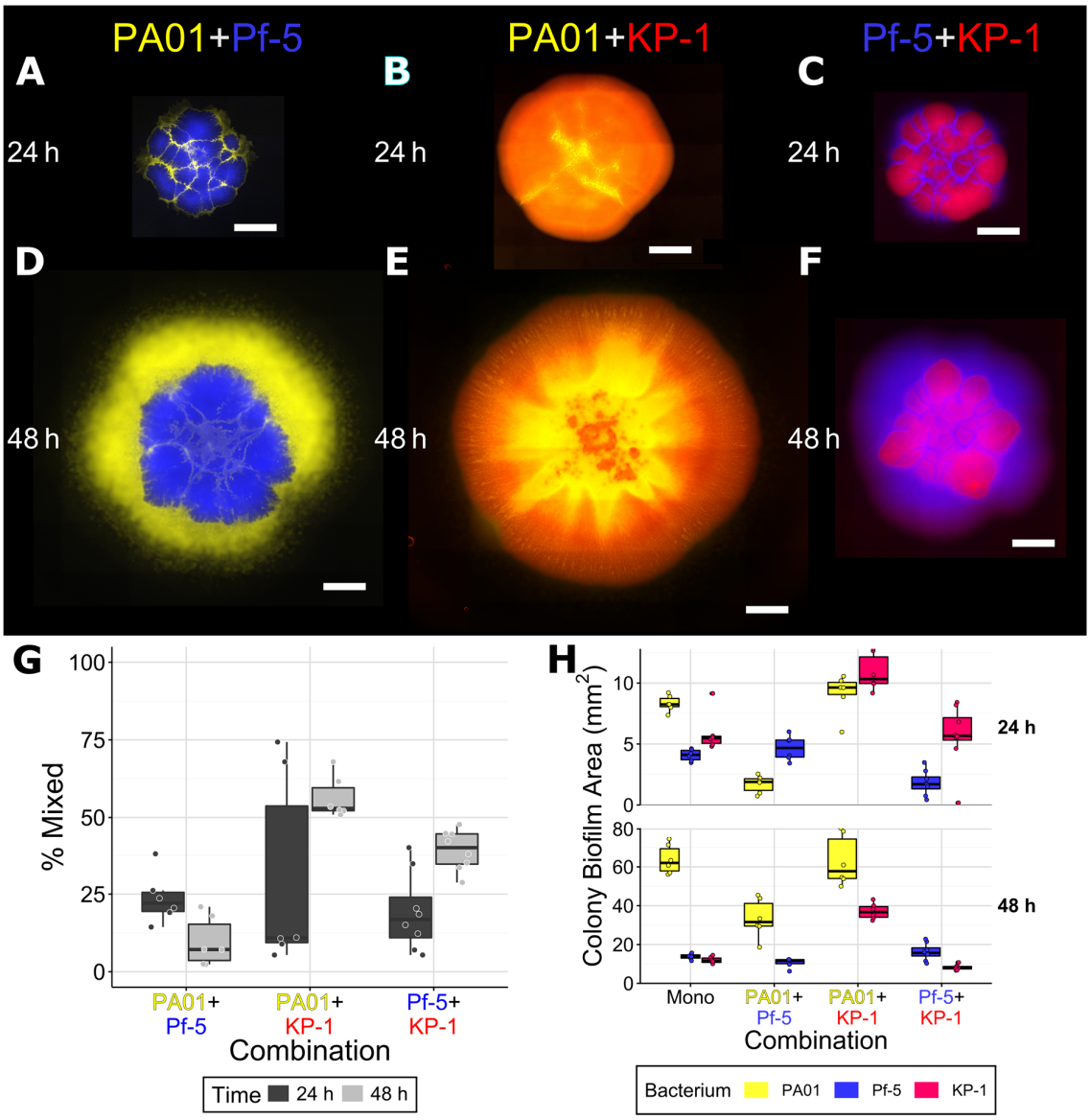

Figure 2: Dual species colonies of *P. aeruginosa* PAO1 and *P. protegens* Pf-5 (A, D), *P. aeruginosa* PAO1 and *K. pneumoniae* KP-1 (B, E), and *P. protegens* Pf-5 and *K. pneumoniae* KP-1 (C, F), overlap between differently labeled strains (G) and the area covered by individual species in colonies (H). Each species was labeled with different fluorescent protein genes and are presented here as yellow (*P. aeruginosa* PAO1), blue (*P. protegens*) and red (*K. pneumoniae*). Strains were mixed 1:1 (OD_{600}) at the time of inoculation and colonies were imaged after 24 and 48 h of growth. Scale bar indicates 1000 µm. Boxplots are presented in Tukey style.

179

180 **Dual Species Colonies**

181 In contrast to monospecies colonies, dual species colonies differed in the area colonized
182 and mixing of species (Figure 2). None of the combinations of species separated into clear
183 radial sectors, as observed for the dual-strain colonies described above, and instead formed
184 distinct patterns. *P. aeruginosa* localized around the perimeter of *P. protegens* colonies (Figure
185 2A,D), especially after 48 h and these species did not mix at either timepoint. While *P.*
186 *aeruginosa* appeared to be restricted to the interior of the colony when cultured with *K.*
187 *pneumoniae* (Figure 2B,E), closer inspection of brightfield images (Supplementary Figure 1)
188 showed that *P. aeruginosa* was also present around the outside perimeter of *K. pneumoniae*, as
189 visible with its distinct lattice morphology. This combination changed from unmixed (~25%,
190 though variable) at 24 h to mixed at 48 h (consistently 50%). When grown with *K. pneumoniae*,
191 *P. protegens* grew around the outer edge of the colony (Figure 2C,F) and these species were
192 also partially mixed (~40%) at 48 h. The amount of area covered by each strain in the dual-
193 species colonies was compared to the area covered by single species colonies (Figure 2, H,
194 Supplementary Table 1). At 24 h, the area covered by *P. aeruginosa* (~8 mm^2) was lower when
195 co-cultured with *P. protegens* (~2 mm^2) and was similarly reduced at 48 h, from ~70 mm^2
196 (monospecies) compared to ~35 mm^2 (dual species). In contrast, there was no difference in the
197 area covered by *P. protegens* when co-cultured with *P. aeruginosa*, although it was
198 significantly decreased (from ~4 to ~1.5 mm^2) at 24 h, but not 48 h, with *K. pneumoniae*. The
199 area covered by *K. pneumoniae* increased when co-cultured with *P. aeruginosa* from ~5 to ~10
200 mm^2 at 24 h and ~12 to ~40 mm^2 at 48 h, but was not affected by *P. protegens.*

201

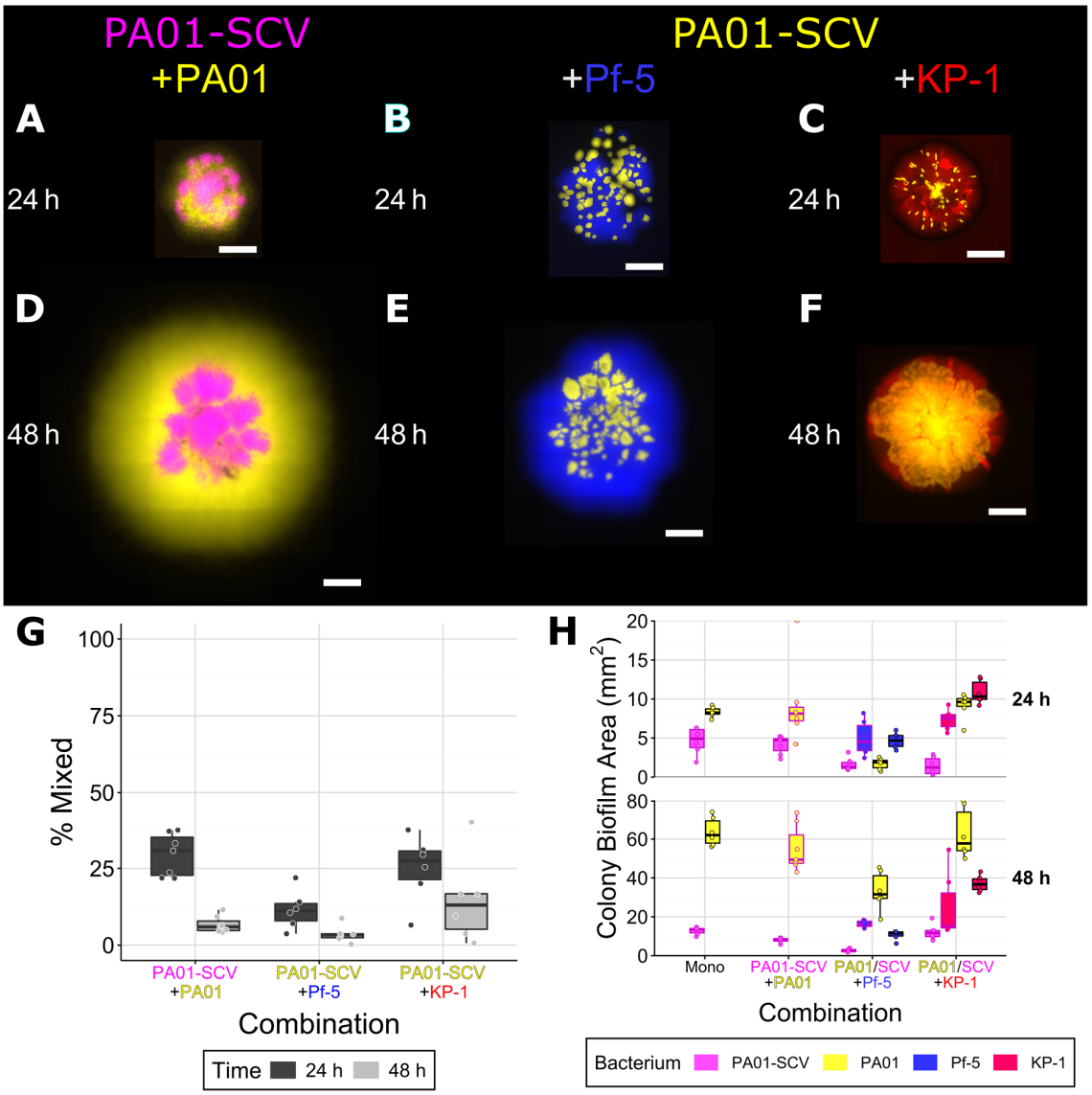

Figure 3: Co-culture colonies consisting of *P. aeruginosa* PAO1 and *P. aeruginosa* PAO1 small colony variant (SCV) (A, D), *P. aeruginosa* PAO1 SCV and *P. protegens* Pf-5 (B, E) and *P. aeruginosa* PAO1 SCV and *K. pneumoniae* KP-1 (C, F), overlap between differently labeled strains (G), and the area covered by individual species/strains (H). Each species was labeled with different fluorescent protein genes and are presented here as yellow (*P. aeruginosa* wild-type when paired with the SCV, SCV when paired with the other two species), magenta (*P. aeruginosa* SCV), blue (*P. protegens*) and red (*K. pneumoniae*). Strains were mixed 1:1 (OD_{600}) at the time of inoculation and colonies were imaged after 24 and 48 h of growth. Scale

211 bar indicates 1000 µm. Boxplots are presented in Tukey style. For the area boxplots (H)
212 combinations of *P. aeruginosa* with *P. protegens* or *K. pneumoniae*, boxes outlined in black
213 represent the wild-type (same data as Figure 2H), outlines in magenta represent combinations
214 with the SCV.
215
216 **Co-cultures with a *P. aeruginosa* Small Colony Variant**
217 To investigate the effect of the type IV pilus (TFP) of *P. aeruginosa* in colonies, a small
218 colony variant (SCV) was cultured in dual species colonies with the parental strain, *P.*
219 *protegens* and *K. pneumoniae*. Based on whole genome sequencing, we previously determined
220 that this SCV differs from the wild-type only by a single mutation in *pilT* [35], preventing pilus
221 retraction and therefore TFP motility [41, 42]. Colonies formed with the SCV differed from
222 those with wild-type *P. aeruginosa* and the mixing of strains/species also differed (Figure 3).
223 Both *P. aeruginosa* (Figure 3A,D) and *P. protegens* (Figure 3B,E) formed a perimeter around
224 the SCV, but there was very little (≤10%) mixing of strains/species. The SCV only mixed
225 slightly more with *K. pneumoniae* (Figure 3C,F). The SCV colonized less area than wild-type
226 *P. aeruginosa,* ~12 mm^2 compared to ~70 mm^2, respectively, after 48 h (Figure 3, H). In dual
227 species colonies, the area covered by the SCV was reduced to ~2 mm^2 at 48 h in the presence
228 of *P. protegens*. When grown with *K. pneumoniae*, the SCV covered less area at 24 h but this
229 was not apparent at 48 h. The SCV did not affect the area covered by the other strains and in
230 contrast to when the parental strain of *P. aeruginosa* was present, the SCV did not increase the
231 area covered by *K. pneumoniae*.

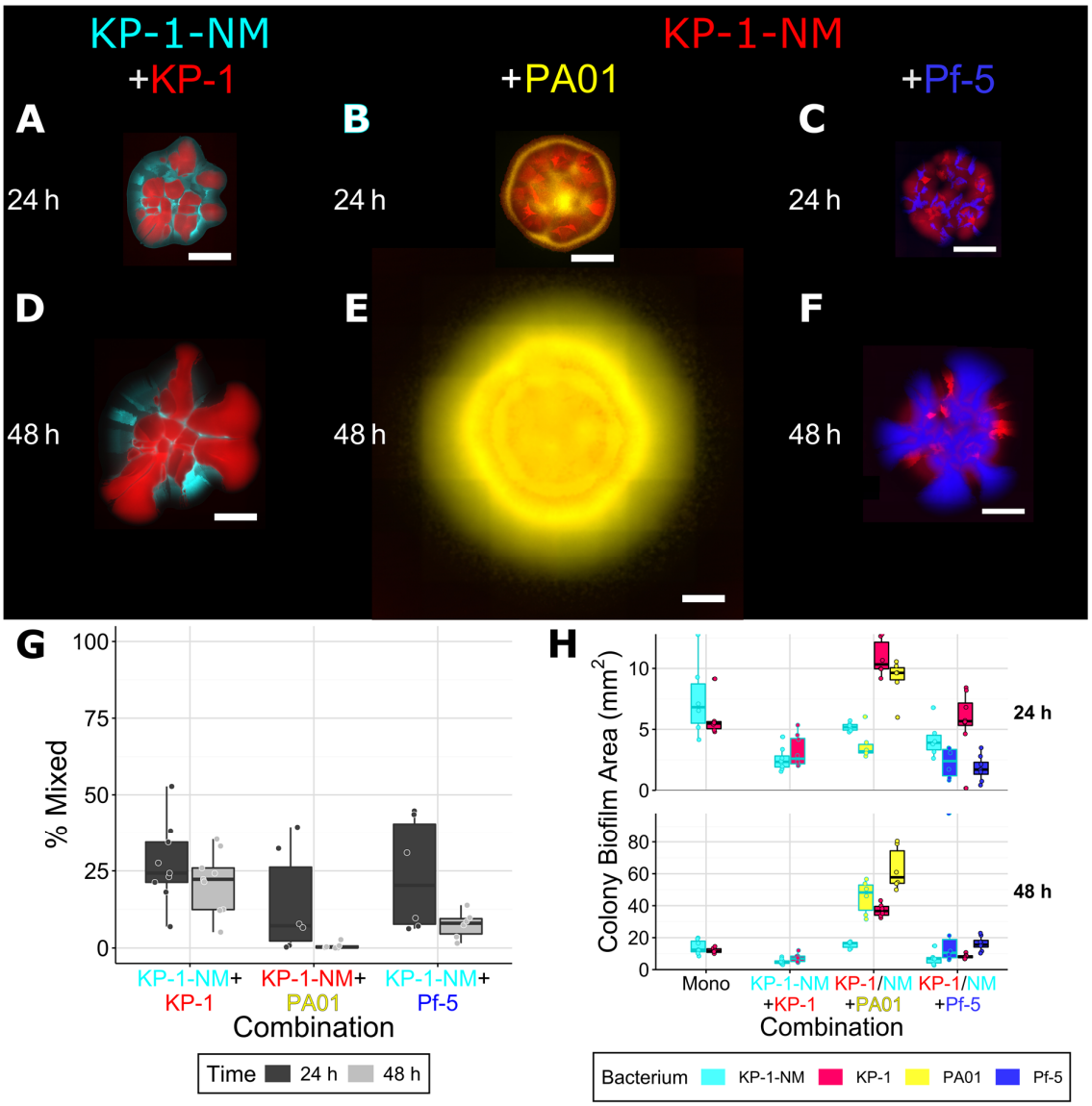

Figure 4: Co-culture colonies consisting of *K. pneumoniae* KP-1 with the *K. pneumoniae* KP-1 non-mucoid variant (NMV) (A, D), *K. pneumoniae* KP-1 NMV with *P. aeruginosa* (B, E), and *K. pneumoniae* KP-1 NMV with PAO1 *P. protegens* Pf-5 (C, F), overlap between differently labeled strains (G) and the area covered by individual species/strains (H). Each species was labeled with different fluorescent protein genes and are presented here as yellow (*P. aeruginosa*), blue (*P. protegens*), red (*K. pneumoniae* wild-type when paired with the NMV, *K. pneumoniae* NMV when paired with the other species) and cyan (*K. pneumoniae* NMV). Strains were mixed 1:1 (OD_{600}) at the time of inoculation and colonies were imaged

241 after 24 and 48 h of growth. Scale bar indicates 1000 µm. Boxplots are presented in Tukey
242 style. For the area boxplots (H), combinations of *K. pneumoniae* with *P. aeruginosa* or *P.*
243 *protegens*, boxes outlined in black represent the wild-type (same data as Figure 2, H), outlines
244 in cyan represent the NMV.
245
246 **Co-cultures with a Non-Mucoid *K. pneumoniae* Variant**
247 To investigate the effects of extracellular matrix (ECM) production by *K. pneumoniae*,
248 a non-mucoid variant (NMV) was cultured in dual strain/species colonies with the parental
249 strain, *P. aeruginosa* and *P. protegens*. This previously characterized NMV has a mutation
250 within a probable colanic acid synthesis gene cluster, preventing it from producing its normal,
251 thick ECM [35]. Single-strain colonies formed by the NMV differed from wild-type *K.*
252 *pneumoniae* (Supplementary Figure 2). Boundaries between sectors of the NMV were jagged
253 instead of straight as was observed for the wild-type. Dual-species colonies with the NMV also
254 differed as it did not mix with wild-type *K. pneumoniae* or *P. protegens* (Figure 4). When
255 grown with *P. aeruginosa* (Figure 4B,E), mixing was low at 24 h (10-20%) and was not readily
256 observed at 48 h. When grown as single-strain colonies, wild-type *K. pneumoniae* and the
257 NMV each covered a similar amount of area. When the two were co-cultured together (Figure
258 4A,D), the NMV covered less area, ~2.5 mm^2, compared to when grown alone, ~7 mm^2, at 24
259 h, and was also reduced at 48 h (from ~12 to ~5 mm^2). The area covered by the NMV was also
260 decreased when paired with *P. protegens* (Figure 4C,F), however, neither of these differences
261 persisted at 48 h. In contrast, the area covered by *P. aeruginosa* was decreased when grown in
262 the presence of the *K. pneumoniae* NMV at 24 h but not 48 h. When paired with *P. aeruginosa*,
263 the area covered by the NMV was not significantly increased as was observed for the parental
264 *K. pneumoniae* strain when paired with *P. aerguinosa*.

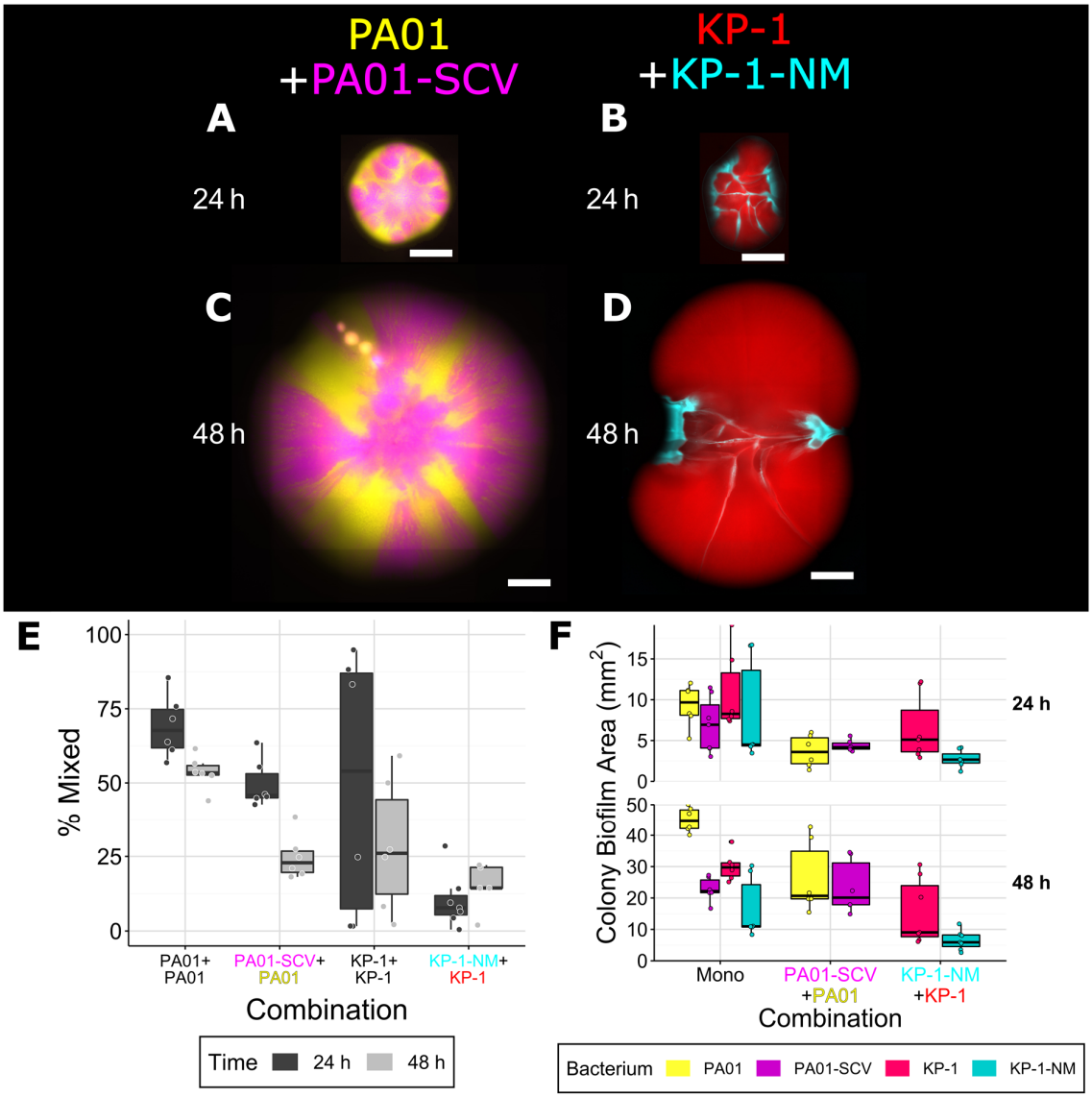

Figure 5: Co-culture colonies on 0.6% agar consisting of *P. aeruginosa* PAO1 with *P. aeruginosa* small colony variant (SCV) (A, C), and *K. pneumoniae* with *K. pneumoniae* KP-1 non-mucoid variant (NMV) (B, D), overlap between differently labeled strains (E) and the area covered by individual species/strains (F). Each species was labeled with different fluorescent protein genes and are presented here as yellow (*P. aeruginosa* wild-type), magenta (*P. aeruginosa* SCV), red (*K. pneumoniae* wild-type) and cyan (*K. pneumoniae* NMV). Strains were mixed 1:1 (OD_{600}) at the time of inoculation and colonies were imaged after 24 and 48 h of growth. Scale bar indicates 1000 µm. Boxplots are Tukey style.

274

275 **Colonies Cultured on 0.6% Agar**

276 The percentage of agar influences motility, as lower percentages enable swarming
277 and/or swimming motility and affect the colony growth of highly mucoid strains [28].
278 Culturing on a lower percentage of agar was thus expected to affect interactions between the
279 wild-type strains of *P. aeruginosa* and *K. pneumoniae* and their non-motile (SCV) and non-
280 mucoid (NMV) variants. Colonies consisting of wild-type and mutant strains grown on 0.6%
281 agar had altered morphologies (Figure 5) and areas colonized (Table 2), but those consisting
282 of two differently labeled wild-type strains did not. Additionally, the wild-type strains did not
283 differ in how they separated into sectors (Supplementary Figure 3). When the *P. aeruginosa*
284 SCV was co-cultured with its parental strain (Figure 5A,C), both strains expanded outwards
285 together, but were less mixed (~22% at 48 h) compared to the two differently coloured wild-
286 type *P. aeruginosa* strains (~55% at 48 h, Figure 1G), which was similar to that observed on
287 1.5% agar (50%, Figure 1G). When the *K. pneumoniae* NMV was co-cultured with the wild-
288 type (Figure 5B,D), the two strains showed little mixing, however by 48 h the wild-type had
289 expanded much more than the NMV (Figure 5, D). When two wild-type *K. pneumoniae* strains
290 were grown together, they mixed comparably on both percentages of agar (~25%, Figure 5E,
291 Figure 1G). Colony area was significantly higher for the *P. aeruginosa* SCV on 0.6% compared
292 to 1.5% agar at 48 h (~20 vs ~10 mm^2, Figure 5F). This was significantly lower than the wild-
293 type on 0.6% agar (~50 mm^2), which was also significantly decreased compared to on 1.5%
294 agar (~70 mm^2). When cultured with the SCV on 0.6% agar, wild-type *P. aeruginosa* area was
295 significantly reduced at both timepoints (from 45 to 22 mm^2 at 48 h). The *K. pneumoniae* wild-
296 type colonized a significantly increased area on 0.6% agar (~27 mm^2) compared to the NMV
297 (~10 mm^2) and the wild-type on 1.5% agar (~11 mm^2). When they were co-cultured, the area
298 colonized by wild-type, but not NMV *K. pneumoniae*, was significantly lower after 48 h.

299

300 Table 2: Comparison of effects of 0.6% agar on colonies of *P. aeruginosa*, *P. aeruginosa* small

301 colony variant (SCV), *K. pneumoniae* and *K. pneumoniae* non-mucoid (NM) variant.

	Wild-type compared to mutant				**Monospecies 0.6% agar**		**Wild-type and mutant 0.6% agar**	
	1.5% Agar		**0.6% Agar**					
Time	24 h	48 h	24 h	48 h	24 h	48 h	24 h	48 h
PAO1	SCV ↓	SCV ↓		SCV ↓		↓	↓	↓
PAO1-SCV						↑		
KP-1				NMV ↓		↑		↓
KP-1-NMV								

302 * Results from comparisons between the wild-type and mutant on each percentage of agar,

303 between agar percentages for each strain and the between cultivation alone or in combination

304 are shown. Interactions that resulted in a significant increase in area are indicated by ↑ and

305 decreases by ↓, using analysis of variance and Tukey's honest significant differences post-

306 hoc test. Differences were considered significant if their multiple-testing adjusted p-value

307 (95% confidence) was below 0.05. Empty cells indicate no significant change.

308

309 **Discussion**

310 **Colonies highlight differences in intraspecies interactions**

311 For each of the three species from our model community, intraspecific competition

312 resulted in species-specific patterns of sector formation. Separation of mixed colonies into

313 sectors has been attributed to genetic drift at the leading edge of the colony, as despite having

314 equal fitness, stochastic effects result in new territory being colonized by either one strain or

315 the other, but not both [43]. Here we show that the shape of the boundaries between sectors
316 depends on the bacterium's physiological traits. The separation of wild-type *K. pneumoniae*
317 strains into sectors with straight boundaries resembled that of *Saccharomyces cerevisiae* [25],
318 whereas the jagged boundaries of *P. protegens* were more similar to those of *P. stutzeri* [27],
319 simulated rod-shaped cells [44] or *E. coli* [43]. In the case of *E. coli*, the formation of fractal
320 boundaries between sectors has been explained by the anisotropic forces of cell division and
321 growth causing unlinked chains of rod-shaped cells to buckle [45]. Thus, similar buckling
322 likely causes the formation of jagged edges between boundaries of the wild-type *P. protegens*
323 strains. The jagged boundaries visible between sectors within *K. pneumoniae* NMV colonies
324 (Supplementary Figure 2) indicate that its secreted extracellular matrix causes the straight
325 boundaries between sectors observed in the wild-type. Colonies of *P. aeruginosa* grown on
326 nutrient rich LB medium were previously shown to be well mixed [46], similar to our
327 observations here using minimal medium. The observation that *pilB* mutants segregate into
328 clear sectors [46] and the resemblance of videos of the edge of *P. aeruginosa* colonies
329 (Supplementary Video 1) to those showing TFP motility [47] indicates that this motility likely
330 enabled the mixing of the *P. aeruginosa* wild-type strains.
331
332 **Interspecies interactions differ from intraspecies interactions**
333 Previous studies have focused on colonies of either identical, but differently labeled
334 strains of the same species, or strains with specific genetic modifications, whereas here, we
335 investigated interactions between different species. While the patterns for our single strain data
336 resemble previous work, it is clear that patterns of species distribution in mixed species
337 colonies differ markedly. Thus, the data presented here show how the different physiological
338 traits of the three studied bacteria determine community composition and spatial distribution
339 in colonies.

340 We have assessed the three pairwise interactions tested here using the notation of
341 Momeni et al. [24], where A [~,~] B indicates a neutral interaction and A[↑,↓]B indicates a
342 relationship where A benefits and B is negatively affected (Table 3). The spatial distribution
343 patterns of *P. aeruginosa* with *P. protegens*, and *P. protegens* with *K. pneumoniae* are similar
344 as one strain expanded outward faster and surrounded the other. Although the area covered by
345 the inner strains was not reduced compared to when they were grown alone, both interactions
346 negatively affect the inner strain as it no longer had equal access to space/nutrients. For the
347 first pair, the area covered by the outer strain, *P. aeruginosa,* was significantly decreased,
348 indicating that both strains experienced negative outcomes from the interaction, so *P.*
349 *aeruginosa* [↓,↓] *P. protegens*. For the second pair, *P. protegens* was the outer strain but its
350 area was not reduced so, *P. protegens* [~,↓] *K. pneumoniae*. In the third case, when *P.*
351 *aeruginosa* was paired with *K. pneumoniae*, *P. aeruginosa* did not differ in the amount of area
352 covered but the area of *K. pneumoniae* was significantly increased, so, *P. aeruginosa* [~,↑] *K.*
353 *pneumoniae*. Consistent with our previous work comparing planktonic and biofilm growth
354 modes, these results differ from our observations in planktonic culture where *P. protegens*
355 outgrew the other two species by between 10-100 fold and *P. aeruginosa* and *K. pneumoniae*
356 equally reduced each other's growth by ~100 fold [22].
357

358 Table 3: Comparison of dual species interactions for *P. aeruginosa*, *P. aeruginosa* small
359 colony variant (SCV), *P. protegens*, *K. pneumoniae* and *K. pneumoniae* non-mucoid variant
360 (NMV).

Recipient / **Actor**	***P. aeruginosa***	***P. aeruginosa* SCV**	***P. protegens***	***K. pneumoniae***	***K. pneumoniae* NMV**
P. aeruginosa				↑	
***P. aeruginosa*-SCV**	↓				ND
P. protegens	↓	↓		↓	
K. pneumoniae					↓
***K. pneumoniae*-NMV**		ND			

361 * Empty cells indicate no difference between single and dual species colonies was observed,
362 ND indicates a combination which was not determined. Interactions that resulted in a
363 significant increase in area are indicated by ↑ and decreases by ↓ compared to the monospecies
364 colony by analysis of variance and Tukey's honest significant differences post-hoc test.
365 Differences were considered significant if their multiple-testing adjusted p-value was below
366 0.05 for 48 h comparisons.
367
368 The interactions between *K. pneumoniae* and the two *Pseudomonas* species were
369 starkly different. When it was grown with *P. aeruginosa* it colonized more than twice as much
370 area than it could alone, indicating a strong benefit from being co-cultured. *P. fluorescens* Pf0-
371 1 has been observed to rapidly evolve a division of labour where two different mutant strains
372 are able to make a faster expanding colony than either the wild-type or each strain individually
373 [48]. In those mixed colonies, one strain produced the force for colony expansion through cell
374 division while the other produced an extracellular polymer which acts as a lubricant at the

375 expanding edge of the colony. In our work, *K. pneumoniae* may have been taking advantage
376 of the extracellular DNA [49] or rhamnolipid surfactants [50] produced by *P. aeruginosa* to
377 enable colony expansion. Non-motile *E. coli* was observed to take advantage of motile
378 *Acinetobacter baylyi,* forming intricately branched floral patterns [51]. These patterns were
379 qualitatively dissimilar to those we observed, indicating that the mechanism by which *K.*
380 *pneumoniae* takes advantage of *P. aeruginosa* motility is also likely different. This strong
381 effect of *P. aeruginosa* on *K. pneumoniae* is consistent with our observations in flow cell
382 biofilms where despite making up only a small (1-5%) proportion of the 3-species community,
383 *P. aeruginosa* influences the relative proportions of both other bacteria [22]. Conversely, *P.*
384 *protegens* did not assist *K. pneumoniae* but was found around the outside of *K. pneumoniae*
385 and these two strains were also more mixed at 48 h than monospecies colonies of each species.
386 In strains of *E. coli* engineered to have equal growth rates but different cell shapes, small cells
387 were found to reside on top of the colonies and larger cells were below, at the agar surface,
388 where they maintained access to nutrients obtained from an agar surface [26]. *K. pneumoniae*
389 cells are larger than *Pseudomonas* which may have allowed *P. protegens* to overgrow it and
390 prevent *K. pneumoniae* from expanding further. In the third case, *P. aeruginosa* was also found
391 around the outside of *P. protegens*, but these species were not mixed. This indicates that *P.*
392 *protegens* could not take advantage of *P. aeruginosa*'s motility and these species mutually
393 exclude each other in space.
394
395 ***P. aeruginosa* twitching motility is important for interactions**
396 Twitching motility by *P. aeruginosa* has been best studied in interstitial biofilms where
397 cells are sandwiched between an agar surface and a glass coverslip [42, 47, 49, 52]. The
398 colonies studied here are qualitatively similar, although the expanding front does not form as
399 intricate lattices. Without a functional TFP, the SCV could only colonize about 20% of the area

400 of the wild-type. When paired with wild-type *P. aeruginosa* or *P. protegens*, the SCV was
401 outcompeted for space, indicating that TFP motility is a competitive trait. It also appears to be
402 a cooperative trait as the area colonized by *K. pneumoniae* was not increased when paired with
403 the *P. aeruginosa* SCV, whereas it was increased three-fold when paired with TFP motile,
404 wild-type *P. aeruginosa*. TFP motility can also be abrogated by deleting the gene for pilin
405 subunits, pilA [52]. It will be interesting to contrast our observations of a hyper-piliated *pilT*
406 mutant with a non-piliated *pilA* mutant. In flow-cell biofilms, a *pilA* mutant of *P. aeruginosa*
407 was less competitive with *Agrobacterium tumefaciens* [53], but conversely, outcompeted
408 *Staphylococcus aureus* [54]. Motility, as a competitive trait, has been suggested to allow strains
409 better access nutrients, to cover other organisms or to disrupt their biofilms [55], which is
410 supported by our results. Even though *P. aeruginosa* was able to cover *K. pneumoniae* with
411 and without a functional TFP, only the motile wild-type *P. aeruginosa* had a commensal
412 relationship with *K. pneumoniae*, indicating that motility can also be a cooperative trait.
413
414 ***K. pneumoniae* secreted matrix is important for interactions**
415 Self-secreted extracellular matrix is a hallmark of biofilms that influences the spatial
416 positioning and interactions between cells within a biofilm [23]. Matrix secretion allows
417 producing cells to better access nutrients in colonies of *P. fluorescens* [56] and for simulated
418 cells under flow conditions [57], by excluding other cells. In flow-cell biofilms, the *K.*
419 *pneumoniae* NMV outcompeted its isogenic wild-type strain, but was less fit when grown with
420 *P. aeruginosa* and *P. protegens* [35]. In colony biofilms, the *K. pneumoniae* NMV colonized
421 the same total area as the wild-type strain when alone, but did not mix when the two were co-
422 cultured. Furthermore, the NMV did not colonize more area when paired with *P. aeruginosa*
423 and was outcompeted by *P. protegens*, resulting in less area covered compared to the NMV
424 when cultured alone. This indicates that the biofilm matrix normally produced by *K.*

425 *pneumoniae* KP-1 improves interspecies, but not [58] intraspecies, competition. The mutual
426 exclusion observed between the wild-type and NMV also indicates that the NMV cannot take
427 advantage of the wild-type, similarly to exclusion by *B. subtilis* [59] and *V. cholerae* [60].
428 When co-cultured, *Pantoea agglomerans* and *B. subtilis* form colonies with structural
429 properties not observed in either single species alone, even with a *B. subtilis* mutant that does
430 not produce EPS, indicating that it could share the exopolysaccharide being produced by *P.*
431 *agglomerans* [58]. Our results indicate that the *K. pneumoniae* NMV can not similarly make
432 use of *Pseudomonas* matrix components.

433

434 **Agar concentration changes inter-strain interaction outcomes**

435 It is well understood that agar concentration influences bacterial motility [61]. It also
436 affects the ability of biofilms to extract nutrients as it determines the osmotic pressure of an
437 environment [28]. Here we showed that lowering the agar concentration from 1.5% to 0.6%
438 increased the area colonized by the TFP motility deficient *P. aeruginosa* SCV, though it was
439 still less than the wild-type. However, in co-culture it colonized as much area as the wild-type
440 and was not encircled by the parental wild-type (Table 3). Conversely, the *K. pneumoniae*
441 NMV was less effective at colonization compared to the wild-type on 0.6% but not 1.5% agar,
442 but was still able to compete with the wild-type when co-cultured in both situations. For the *P.*
443 *aeruginosa* SCV, lowering the agar concentration likely enabled flagella-based motility that
444 could partially compensate for the defect in twitching motility. Motility is important for
445 colonization of roots [62], the gastrointestinal tract of Zebra fish [63] and for the persistence
446 of uropathogenic *E. coli* [64]. Here, we showed that motility influenced intraspecies
447 competition but the outcome depended on environmental conditions. Previously, we observed
448 that the *P. aeruginosa* SCV completely outcompeted wild-type *P. aeruginosa* in flow cell
449 biofilms [35]. The increased attachment provided by hyper-piliation of the SCV [42, 65] likely

450 provides this benefit in flow cells, whereas the lack of motility was a detriment in colonies.
451 This highlights the differences in environmental pressures between the culturing methods.
452 Hyper-piliation also leads to aggregation [66], which may explain how the *P. aeruginosa* wild-
453 type and SCV separated into sectors with straight boundaries on 0.6% agar. This appeared to
454 be similar to the differently tagged strains of *K. pneumoniae*, indicating that this community
455 morphology may not exclusively be caused by matrix secretion.

456 For *K. pneumoniae* (which is non-motile), lowering the agar concentration allowed the
457 wild-type to colonize more area, which was similar to how a rugose strain of *V. cholerae* that
458 hypersecretes extracellular matrix (ECM)formed larger colonies on lower concentrations of
459 agar [28]. In *V. cholerae*, it was demonstrated that matrix secretion generates an osmotic
460 pressure gradient between the agar and the colony, allowing the colony to expand by physical
461 swelling and also drawing more nutrients out of the agar. It is likely that this is a general
462 mechanism attributable to the biofilm matrix. In this context, the wild-type *K. pneumoniae*
463 would be similar to the rugose *V. cholerae*, producing larger amounts of ECM, while the *K.*
464 *pneumoniae* NMV and wild-type *V. cholerae* are analogous in their relatively lower amount of
465 ECM production. The community morphology of dual strain colonies of ECM secretors and
466 non-secretors differed between the two species. In *V. cholerae*, the hyper-secretor was
467 encircled by the non-secretor at both 1.5 and 0.6% agar, but colonized far more area at 0.6%
468 as the non-secretor was pushed to the outside of the colony. Conversely, the *K. pneumoniae*
469 NMV was not displaced and even prevented spreading by wild-type *K. pneumoniae* (Figure 5,
470 D). Similar to *V. cholerae*, the *K. pneumoniae* NMV did not benefit from the matrix secreted
471 by wild-type *K. pneumoniae* as its area was not increased in co-culture. In *B. subtilis*, it was
472 also observed that ECM-producing cells outcompete non-secretors [29], and to a higher degree
473 when the humidity is higher (which is similar to lower agar concentration). Additionally,
474 osmotic pressure generated by the ECM enhances colony spreading in this species [67]. Thus,

475 matrix production appears to be a general strategy of bacteria that increases competitiveness in
476 colonies.
477
478 **Conclusions**
479 Interactions between bacteria are key for determining the composition and function of
480 communities. Here we used colonies to investigate intra- and inter-species interactions. Using
481 the members of our three species model community, we showed that they differ in how they
482 interact with members of their own species due to their physiological traits: TFP motility in *P.*
483 *aeruginosa* allowed populations to mix whereas ECM in *K. pneumoniae* caused straight
484 borders between population sectors. Using mutants deficient in these traits, we showed that
485 their impact depended on the agar concentration. These physiological traits were also important
486 when interspecies interactions were examined. The motility of *P. aeruginosa* enabled it to
487 outcompete *P. protegens* and to facilitate increased colonization area by *K. pneumoniae*.
488 Importantly, the spatial distribution of species, observed for dual-species colonies did not
489 resemble any patterns previously seen for experimental or simulated monospecies and dual-
490 strain colonies. These experiments show that interspecies interactions differ substantially from
491 intraspecies interactions and that co-culture colonies are a powerful way to investigate how
492 bacterial physiology determines these interactions.
493

Acknowledgments

The authors would like to thank Sujatha Subramoni for helpful advice regarding the three species community, Talgat Sailov for microscopy assistance and Diane McDougald for reading the manuscript and providing helpful comments. We would also like to thank the Singapore Centre for Environmental Life Sciences Engineering (SCELSE), whose research is supported by the National Research Foundation Singapore, Ministry of Education, Nanyang Technological University and National University of Singapore, under its Research Centre of Excellence Programme.

Conflict of Interest

The authors state that they have no conflict of interest.

506 **References**

507 1. Elias S, Banin E (2012) Multi-species biofilms: living with friendly neighbors. FEMS
508 Microbiol Rev 36:990–1004. https://doi.org/10.1111/j.1574-6976.2012.00325.x.

509 2. Rendueles O, Ghigo J-M (2012) Multi-species biofilms: how to avoid unfriendly
510 neighbors. FEMS Microbiol Rev 36:972–989. https://doi.org/10.1111/j.1574-
511 6976.2012.00328.x

512 3. Ghoul M, Mitri S (2016) The Ecology and Evolution of Microbial Competition.
513 Trends Microbiol 24:833–845. https://doi.org/10.1016/j.tim.2016.06.011

514 4. Morris BEL, Henneberger R, Huber H, Moissl-Eichinger C (2013) Microbial
515 syntrophy: interaction for the common good. FEMS Microbiol Rev 37:384–406.
516 https://doi.org/10.1111/1574-6976.12019

517 5. Cornforth DM, Foster KR (2015) Antibiotics and the art of bacterial war. Proc Natl
518 Acad Sci U S A 112:10827–8. https://doi.org/10.1073/pnas.1513608112

519 6. Sharma A, Inagaki S, Sigurdson W, Kuramitsu HK (2005) Synergy between
520 Tannerella forsythia and Fusobacterium nucleatum in biofilm formation. Oral
521 Microbiol Immunol 20:39–42. https://doi.org/10.1111/j.1399-302X.2004.00175.x

522 7. Yamada M, Ikegami A, Kuramitsu HK (2005) Synergistic biofilm formation by
523 *Treponema denticola* and *Porphyromonas gingivalis*. FEMS Microbiol Lett 250:271–
524 277. https://doi.org/10.1016/j.femsle.2005.07.019

525 8. Gonzalez D, Sabnis A, Foster KR, Mavridou DAI (2018) Costs and benefits of
526 provocation in bacterial warfare. Proc Natl Acad Sci 115:7593–7598.
527 https://doi.org/10.1073/pnas.1801028115

528 9. Cordero OX, Datta MS (2016) Microbial interactions and community assembly at

529 microscales. Curr Opin Microbiol 31:227–234.
530 https://doi.org/10.1016/J.MIB.2016.03.015

531 10. Abreu NA, Taga ME (2016) Decoding molecular interactions in microbial
532 communities. FEMS Microbiol Rev 40:648–663.
533 https://doi.org/10.1093/femsre/fuw019

534 11. Madsen JS, Sørensen SJ, Burmølle M (2018) Bacterial social interactions and the
535 emergence of community-intrinsic properties. Curr Opin Microbiol 42:104–109.
536 https://doi.org/10.1016/J.MIB.2017.11.018

537 12. Foster KR, Bell T (2012) Competition, not cooperation, dominates interactions among
538 culturable microbial species. Curr Biol 22:1845–1850.
539 https://doi.org/10.1016/j.cub.2012.08.005

540 13. Russel J, Røder HL, Madsen JS, et al (2017) Antagonism correlates with metabolic
541 similarity in diverse bacteria. Proc Natl Acad Sci U S A 114:10684–10688.
542 https://doi.org/10.1073/pnas.1706016114

543 14. Ren D, Madsen JS, Sørensen SJ, Burmølle M (2015) High prevalence of biofilm
544 synergy among bacterial soil isolates in cocultures indicates bacterial interspecific
545 cooperation. ISME J 9:81–89. https://doi.org/10.1038/ismej.2014.96

546 15. Burmølle M, Webb JS, Rao D, et al (2006) Enhanced biofilm formation and increased
547 resistance to antimicrobial agents and bacterial invasion are caused by synergistic
548 interactions in multispecies biofilms. Appl Environ Microbiol 72:3916–23.
549 https://doi.org/10.1128/AEM.03022-05

550 16. Tan CH, Lee KWK, Burmølle M, et al (2017) All together now: experimental
551 multispecies biofilm model systems. Environ Microbiol 19:42–53.

552 https://doi.org/10.1111/1462-2920.13594

553 17. Røder HL, Sørensen SJ, Burmølle M (2016) Studying Bacterial Multispecies Biofilms:
554 Where to Start? Trends Microbiol 24:503–513.
555 https://doi.org/10.1016/j.tim.2016.02.019

556 18. Dragoš A, Kiesewalter H, Martin M, et al (2018) Division of Labor during Biofilm
557 Matrix Production. Curr Biol 28:1903-1913.e5.
558 https://doi.org/10.1016/J.CUB.2018.04.046

559 19. Hansen SK, Rainey PB, Haagensen JAJ, Molin S (2007) Evolution of species
560 interactions in a biofilm community. Nature 445:533–536.
561 https://doi.org/10.1038/nature05514

562 20. Haagensen JAJ, Hansen SK, Christensen BB, et al (2015) Development of Spatial
563 Distribution Patterns by Biofilm Cells. Appl Environ Microbiol 81:6120–8.
564 https://doi.org/10.1128/AEM.01614-15

565 21. Christensen BB, Haagensen JAJ, Heydorn A, Molin S (2002) Metabolic
566 commensalism and competition in a two-species microbial consortium. Appl Environ
567 Microbiol 68:2495–502. https://doi.org/10.1128/aem.68.5.2495-2502.2002

568 22. Lee KWK, Periasamy S, Mukherjee M, et al (2014) Biofilm development and
569 enhanced stress resistance of a model, mixed-species community biofilm. ISME J
570 8:894–907. https://doi.org/10.1038/ismej.2013.194

571 23. Nadell CD, Drescher K, Foster KR (2016) Spatial structure, cooperation and
572 competition in biofilms. Nat Rev Microbiol 14:589–600.
573 https://doi.org/10.1038/nrmicro.2016.84

574 24. Momeni B, Shou W, Brileya KA, Fields MW (2013) Strong inter-population

575 cooperation leads to partner intermixing in microbial communities. Elife 2013:e00230.
576 https://doi.org/10.7554/eLife.00230

577 25. Müller MJI, Neugeboren BI, Nelson DR, Murray AW (2014) Genetic drift opposes
578 mutualism during spatial population expansion. Proc Natl Acad Sci U S A 111:1037–
579 42. https://doi.org/10.1073/pnas.1313285111

580 26. Smith WPJ, Davit Y, Osborne JM, et al (2017) Cell morphology drives spatial
581 patterning in microbial communities. Proc Natl Acad Sci U S A 114:E280–E286.
582 https://doi.org/10.1073/pnas.1613007114

583 27. Goldschmidt F, Regoes RR, Johnson DR (2017) Successive range expansion promotes
584 diversity and accelerates evolution in spatially structured microbial populations. ISME
585 J 11:2112–2123. https://doi.org/10.1038/ismej.2017.76

586 28. Yan J, Nadell CD, Stone HA, et al (2017) Extracellular-matrix-mediated osmotic
587 pressure drives Vibrio cholerae biofilm expansion and cheater exclusion. Nat Commun
588 8:327. https://doi.org/10.1038/s41467-017-00401-1

589 29. van Gestel J, Weissing FJ, Kuipers OP, Kovács ÁT (2014) Density of founder cells
590 affects spatial pattern formation and cooperation in Bacillus subtilis biofilms. ISME J
591 8:2069–2079. https://doi.org/10.1038/ismej.2014.52

592 30. Frost I, Smith WPJ, Mitri S, et al (2018) Cooperation, competition and antibiotic
593 resistance in bacterial colonies. ISME J 12:1582–1593.
594 https://doi.org/10.1038/s41396-018-0090-4

595 31. Ramette A, Frapolli M, Saux MF Le, et al (2011) Pseudomonas protegens sp. nov.,
596 widespread plant-protecting bacteria producing the biocontrol compounds 2,4-
597 diacetylphloroglucinol and pyoluteorin. Syst Appl Microbiol 34:180–188.

598 https://doi.org/10.1016/j.syapm.2010.10.005

599 32. Lim CK, Hassan KA, Penesyan A, et al (2013) The effect of zinc limitation on the
600 transcriptome of *Pseudomonas protegens* Pf-5. Environ Microbiol 15:702–715.
601 https://doi.org/10.1111/j.1462-2920.2012.02849.x

602 33. Chazal PM (1995) Pollution of modern metalworking fluids containing biocides by
603 pathogenic bacteria in France. Eur J Epidemiol 11:1–7.
604 https://doi.org/10.1007/BF01719939

605 34. Anand AAP, Vennison SJ, Sankar SG, et al (2010) Isolation and Characterization of
606 Bacteria from the Gut of *Bombyx mori* that Degrade Cellulose, Xylan, Pectin and
607 Starch and Their Impact on Digestion. J Insect Sci 10:1–20.
608 https://doi.org/10.1673/031.010.10701

609 35. Kelvin Lee KW, Hoong Yam JK, Mukherjee M, et al (2016) Interspecific diversity
610 reduces and functionally substitutes for intraspecific variation in biofilm communities.
611 ISME J 10:846–857. https://doi.org/10.1038/ismej.2015.159

612 36. Peng T, Thorn K, Schroeder T, et al (2017) A BaSiC tool for background and shading
613 correction of optical microscopy images. Nat Commun 8:14836.
614 https://doi.org/10.1038/ncomms14836

615 37. Preibisch S, Saalfeld S, Tomancak P (2009) Globally optimal stitching of tiled 3D
616 microscopic image acquisitions. Bioinformatics 25:1463–5.
617 https://doi.org/10.1093/bioinformatics/btp184

618 38. Schneider CA, Rasband WS, Eliceiri KW (2012) NIH Image to ImageJ: 25 years of
619 image analysis. Nat Methods 9:671–675. https://doi.org/10.1038/nmeth.2089

620 39. Barthelme S (2018) imager: Image Processing Library Based on “CImg”.

621 40. Landini G, Randell DA, Fouad S, Galton A (2017) Automatic thresholding from the
622 gradients of region boundaries. J Microsc 265:185–195.
623 https://doi.org/10.1111/jmi.12474

624 41. Whitchurch CB, Hobbs M, Livingston SP, et al (1991) Characterisation of a
625 Pseudomonas aeruginosa twitching motility gene and evidence for a specialised
626 protein export system widespread in eubacteria. Gene 101:33–44.
627 https://doi.org/10.1016/0378-1119(91)90221-V

628 42. Whitchurch CB, Mattick JS (1994) Characterization of a gene, pilU, required for
629 twitching motility but not phage sensitivity in Pseudomonas aeruginosa. Mol
630 Microbiol 13:1079–1091. https://doi.org/10.1111/j.1365-2958.1994.tb00499.x

631 43. Hallatschek O, Hersen P, Ramanathan S, Nelson DR (2007) Genetic drift at expanding
632 frontiers promotes gene segregation. Proc Natl Acad Sci U S A 104:19926–30.
633 https://doi.org/10.1073/pnas.0710150104

634 44. Blanchard AE, Lu T (2015) Bacterial social interactions drive the emergence of
635 differential spatial colony structures. BMC Syst Biol 9:59.
636 https://doi.org/10.1186/s12918-015-0188-5

637 45. Rudge TJ, Federici F, Steiner PJ, et al (2013) Cell Polarity-Driven Instability
638 Generates Self-Organized, Fractal Patterning of Cell Layers. ACS Synth Biol 2:705–
639 714. https://doi.org/10.1021/sb400030p

640 46. Mitri S, Clarke E, Foster KR (2016) Resource limitation drives spatial organization in
641 microbial groups. ISME J 10:1471–1482. https://doi.org/10.1038/ismej.2015.208

642 47. Gloag ES, Turnbull L, Huang A, et al (2013) Self-organization of bacterial biofilms is
643 facilitated by extracellular DNA. Proc Natl Acad Sci U S A 110:11541–6.

644 https://doi.org/10.1073/pnas.1218898110

645 48. Kim W, Levy SB, Foster KR (2016) Rapid radiation in bacteria leads to a division of
646 labour. Nat Commun 7:10508. https://doi.org/10.1038/ncomms10508

647 49. Turnbull L, Toyofuku M, Hynen AL, et al (2016) Explosive cell lysis as a mechanism
648 for the biogenesis of bacterial membrane vesicles and biofilms. Nat Commun 7:11220.
649 https://doi.org/10.1038/ncomms11220

650 50. Murray TS, Kazmierczak BI (2008) Pseudomonas aeruginosa exhibits sliding motility
651 in the absence of type IV pili and flagella. J Bacteriol 190:2700–8.
652 https://doi.org/10.1128/JB.01620-07

653 51. Xiong L, Cao Y, Cooper R, et al (2020) Flower-like patterns in multi-species bacterial
654 colonies. Elife. https://doi.org/10.7554/eLife.48885

655 52. Semmler ABT, Whitchurch CB, Mattick JS (1999) A re-examination of twitching
656 motility in Pseudomonas aeruginosa. Microbiology 145:2863–2873.
657 https://doi.org/10.1099/00221287-145-10-2863

658 53. An D, Danhorn T, Fuqua C, Parsek MR (2006) Quorum sensing and motility mediate
659 interactions between Pseudomonas aeruginosa and Agrobacterium tumefaciens in
660 biofilm cocultures. Proc Natl Acad Sci 103:3828–33.
661 https://doi.org/10.1073/pnas.0511323103

662 54. Yang L, Liu Y, Markussen T, et al (2011) Pattern differentiation in co-culture biofilms
663 formed by *Staphylococcus aureus* and *Pseudomonas aeruginosa*. FEMS Immunol
664 Med Microbiol 62:339–347. https://doi.org/10.1111/j.1574-695X.2011.00820.x

665 55. Rendueles O, Ghigo J-MJ-M (2015) Mechanisms of competition in biofilm
666 communities. Microbiol Spectr 3:. https://doi.org/10.1128/microbiolspec.MB-0009-

667 2014

668 56. Kim W, Racimo F, Schluter J, et al (2014) Importance of positioning for microbial
669 evolution. Proc Natl Acad Sci U S A 111:E1639-47.
670 https://doi.org/10.1073/pnas.1323632111

671 57. Jayathilake PG, Jana S, Rushton S, et al (2017) Extracellular Polymeric Substance
672 Production and Aggregated Bacteria Colonization Influence the Competition of
673 Microbes in Biofilms. Front Microbiol 8:1865.
674 https://doi.org/10.3389/fmicb.2017.01865

675 58. Yannarell SM, Grandchamp GM, Chen SY, et al (2019) A dual-species biofilm with
676 emergent mechanical and protective properties. In: Journal of Bacteriology

677 59. Martin M, Dragoš A, Hölscher T, et al (2017) De novo evolved interference
678 competition promotes the spread of biofilm defectors. Nat Commun 8:15127.
679 https://doi.org/10.1038/ncomms15127

680 60. Nadell CD, Drescher K, Wingreen NS, Bassler BL (2015) Extracellular matrix
681 structure governs invasion resistance in bacterial biofilms. ISME J 9:1700–1709.
682 https://doi.org/10.1038/ismej.2014.246

683 61. Greenberg EP, Canale-Parola E (1977) Motility of flagellated bacteria in viscous
684 environments. J Bacteriol 132:356–8

685 62. Pliego C, de Weert S, Lamers G, et al (2008) Two similar enhanced root-colonizing
686 *Pseudomonas* strains differ largely in their colonization strategies of avocado roots and
687 *Rosellinia necatrix* hyphae. Environ Microbiol 10:3295–3304.
688 https://doi.org/10.1111/j.1462-2920.2008.01721.x

689 63. Stephens WZ, Wiles TJ, Martinez ES, et al (2015) Identification of Population

690 Bottlenecks and Colonization Factors during Assembly of Bacterial Communities
691 within the Zebrafish Intestine. MBio 6:e01163-15.
692 https://doi.org/10.1128/mBio.01163-15

693 64. Wright KJ, Seed PC, Hultgren SJ (2005) Uropathogenic Escherichia coli flagella aid in
694 efficient urinary tract colonization. Infect Immun 73:7657–68.
695 https://doi.org/10.1128/IAI.73.11.7657-7668.2005

696 65. Chiang P, Burrows LL (2003) Biofilm formation by hyperpiliated mutants of
697 Pseudomonas aeruginosa. J Bacteriol 185:2374–8.
698 https://doi.org/10.1128/JB.185.7.2374-2378.2003

699 66. Déziel E, Comeau Y, Villemur R (2001) Initiation of biofilm formation by
700 Pseudomonas aeruginosa 57RP correlates with emergence of hyperpiliated and highly
701 adherent phenotypic variants deficient in swimming, swarming, and twitching
702 motilities. J Bacteriol 183:1195–1204. https://doi.org/10.1128/JB.183.4.1195-
703 1204.2001

704 67. Seminara A, Angelini TE, Wilking JN, et al (2012) Osmotic spreading of Bacillus
705 subtilis biofilms driven by an extracellular matrix. Proc Natl Acad Sci.
706 https://doi.org/10.1073/pnas.1109261108

707

708